Supramolecular Chemistry
Publication details, including instructions for authors and subscription information:
http://www.informaworld.com/smpp/title~content=t713649759

p-tert-Butylcalix[4]arene Functionalised with Bipyridyl Carboxylates for Lanthanide Complexation: Synthesis, Photophysical Properties, Solution and Solid State Behavior

Raymond F. Ziessel[a]; LoÏc J. Charbonnière[a]; Michèle Cesario[b]; Thierry Prangé[c]; Massimo Guardigli[d]; Aldo Roda[d]; Alain Van Dorsselaer[e]; Hélène Nierengarten[e]
[a] Laboratoire de Chimie Moléculaire, ESA-au CNRS, ECPM, Strasbourg Cedex 02, France [b] Institut de Chimie des Substances Naturelles, CNRS, Gif-sur-Yvette, France [c] LURE, Bât. 209d, Université Paris-Sud, Paris, France [d] Department of Pharmaceutical Sciences, University of Bologna, Bologna, Italy [e] Laboratoire de Spectrométrie de Masse Bio-organique, ECPM, Strasbourg Cedex 02, France

To cite this Article Ziessel, Raymond F. , Charbonnière, LoÏc J. , Cesario, Michèle , Prangé, Thierry , Guardigli, Massimo , Roda, Aldo , Van Dorsselaer, Alain and Nierengarten, Hélène(2003) '*p-tert*-Butylcalix[4]arene Functionalised with Bipyridyl Carboxylates for Lanthanide Complexation: Synthesis, Photophysical Properties, Solution and Solid State Behavior', Supramolecular Chemistry, 15: 4, 277 — 289

To link to this Article: DOI: 10.1080/1061027021000057224

URL: http://dx.doi.org/10.1080/1061027021000057224

Supramolecular Chemistry, 2003 VOL. 15 (4), pp. 277–289

Taylor & Francis
Taylor & Francis Group

p-tert-Butylcalix[4]arene Functionalised with Bipyridyl Carboxylates for Lanthanide Complexation: Synthesis, Photophysical Properties, Solution and Solid State Behavior

RAYMOND F. ZIESSEL[a,*], LOÏC J. CHARBONNIÈRE[a], MICHÈLE CESARIO[b], THIERRY PRANGÉ[c], MASSIMO GUARDIGLI[d], ALDO RODA[d], ALAIN VAN DORSSELAER[e] and HÉLÈNE NIERENGARTEN[e]

[a]*Laboratoire de Chimie Moléculaire, ESA-7008 au CNRS, ECPM, 25 rue Becquerel, 67087 Strasbourg Cedex 02, France;* [b]*Institut de Chimie des Substances Naturelles, CNRS, F-91128 Gif-sur-Yvette, France;* [c]*LURE, Bât. 209d, Université Paris-Sud, BP 34, F-91898 Orsay Cedex, France and LCRB (UMR 8015 CNRS) Faculté de Pharmacie, 4 Av de l'Observatoire, F-75006 Paris, France;* [d]*Department of Pharmaceutical Sciences, University of Bologna, Via Belmeloro 6, 40126 Bologna, Italy;* [e]*Laboratoire de Spectrométrie de Masse Bio-organique, ECPM, 25 rue Becquerel, 67087 Strasbourg Cedex 02, France*

Received (in Austin, USA) 5 June 2002; Accepted 4 October 2002

A new ligand based on a *p-tert*-butylcalix[4]arene functionalised with three 6-carboxylato-2,2′-bipyridine arms reacted with lanthanide(III) cations to form 2:2 complexes in the solid state, whereas in solution, a concentration-dependent equilibrium is observed between 2:2 and 1:1 species, as evidenced by ES-MS and metal luminescence measurements. In the X-ray molecular structure of the terbium complex two branched calixarene platforms share one pendant arm in order to provide a neutral dimeric structure which is held together by a strong hydrogen bonded network together with efficient $\pi-\pi$ stacking of two pyridine rings belonging to each ligand.

Keywords: Calix[4]arene; Bipyridine-carboxylate; Luminescence; Lanthanide complexes; ES-MS and X-ray structure

INTRODUCTION

The use of functionalised calix[*n*]arenes as receptors for complexation of lanthanide(III) cations has been driven by two major topics: the search for efficient light converting molecular devices [1] and improvement of extraction efficiency in nuclear waste management [2]. In both cases, the calixarenes are expected to afford a well defined preorganized architecture and synthetic modifications at the upper or lower rim allows for functionalisation at will. It is thus possible to focus synthetic efforts toward the linking of suitable arms, depending on the desired property. Calixarenes derivatized with phosphine oxide arms have shown very promising properties regarding their ability to extract lanthanides [3], a crucial step toward the purification of nuclear waste by transmutation. Similarly, the introduction of suitable chromophores as appended [4] or chelating arms [5] leads to highly luminescent complexes of europium and terbium. Unfortunately, these complexes often display poor solubility and stability in aqueous solutions, a necessary prerequisite for their use as luminescent labels in fluoroimmunoassays [6]. Furthermore, chromophoric complexes may also have several applications, such as luminescent probes in biomedical assays [7], luminescent sensors for chemical species (oxygen, halide ions, OH^-, H^+) [8] and electroluminescent devices [9]. Calixarene scaffoldings have previously been used to encapsulate luminescent lanthanide cations [10,11].

In the course of our work on the synthesis of luminescent complexes, we have been interested in the functionalization of three phenolic positions of *p-tert*-butylcalix[4]arene by 6-carboxy-2,2′-bipyridine arms. In their anionic form, such chelating arms are expected to be strongly coordinated to lanthanide cations by forming two five-membered chelating rings per arm, providing neutral complexes. We here describe the synthesis of compound **L** and its coordination behavior with Eu, Gd and Tb in solution, as well as the metal luminescence properties

---

*Corresponding author. E-mail: ziessel@chimie.u-strasbg.fr

ISSN 1061-0278 print/ISSN 1029-0478 online © 2003 Taylor & Francis Ltd
DOI: 10.1080/1061027021000057224

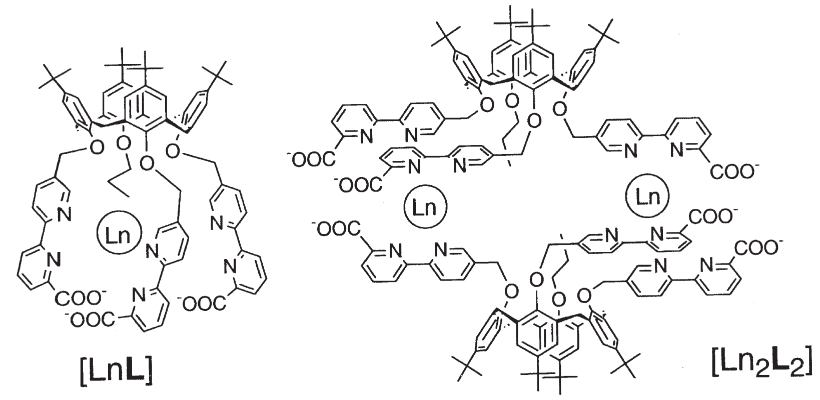

SCHEME 1

and the X-ray crystal structure of the terbium complex. The coordination features of ligand **L** are illustrated in Scheme 1.

EXPERIMENTAL

General Methods

The 200.1 (^{1}H) and 50.3 MHz (^{13}C) NMR spectra were recorded at room temperature on a Bruker AC 200 spectrometer, using perdeuteriated solvents as internal standards: δ(H) in ppm relative to residual protiated solvent or *t*-BuOH ($\delta = 1.30$ ppm) for D_2O solutions; δ(C) in ppm relative to the solvent or to *t*-BuOH ($\delta = 31.6$ and 68.7 ppm) for D_2O solutions. FT-IR spectra were recorded as KBr pellets on a Nicolet 210 spectrometer. High resolution mass spectral analysis (HRMS) was performed using a Mariner ESI-ToF instrument from Applied Bio-Systems/Perkin Elmer. Melting points were obtained on a Büchi 535 capillary melting point apparatus in open-ended capillaries and are uncorrected. Chromatographic purification was conducted using 0.063–0.200 mm silica gel or standardized aluminium oxide 90 obtained from Merck. Thin layer chromatography (TLC) was performed on silica or aluminium oxide plates (Merck) coated with fluorescent indicator. All mixtures of solvents are given in v/v ratios.

Materials

6-Bromo-5′-bromomethyl-2,2′-bipyridine **1** [12], and 5,11,17,23-tetra(*tert*-butyl)-25-propoxycalix[4]arene **2** [13] were prepared according to literature procedures. CH_2Cl_2 (Prolabo) was distilled from CaH_2. THF (Riedel-de-Haën) was dried over Na/benzophenone prior to distillation. CH_3CN (Riedel-de-Haën) was filtered through aluminium oxide (Merck, Act III) and distilled from P_2O_5. [Pd(PPh$_3$)-Cl$_2$] (Aldrich) was recrystallized from hot DMSO.

Synthesis

5,11,17,23-Tetra(tert-butyl)-26,27,28-tris[6-bromo-2,2′-bipyridin-5′-yl]-25-propoxycalix[4]arene (3)

In a Schlenk tube under argon, derivative **2** (280 mg, 0.40 mmol) was dissolved in 20 ml freshly distilled DMF and NaH (60% in mineral oil, 75 mg, 1.87 mmol) was added. The solution was heated to 80°C for 24 hours and compound **1** (465 mg, 1.42 mmol) was added as a solid. Heating was continued for 40 hours resulting in a deep brown solution. After addition of 1 ml water, the solvents were removed under reduced pressure. The residue was partitioned between 50 ml water and 50 ml CH_2Cl_2. The aqueous layer was further washed with two 50 ml portions of CH_2Cl_2 and the combined organic layers were dried over $MgSO_4$ and evaporated to dryness. Purification by column chromatography (Al_2O_3, CH_2Cl_2/hexane, 50/50 to 80/20) followed by recrystallization with a CH_2Cl_2/MeOH mixture and drying under vacuum gave compound **3** (220 mg, 0.15 mmol, 38%) as white crystals. $R_f = 0.43$, Al_2O_3, CH_2Cl_2/hexane, 80/20. ^{1}H NMR ($CDCl_3$): δ 0.81 (t, 3H, $^3J = 7.0$ Hz), 1.08 (s, 18H), 1.11 (s, 9H), 1.12 (s, 9H), 1.77 (m, 2H), 2.95 (d, 2H, $^2J = 12.5$ Hz), 3.08 (d, 2H, $^2J = 12.5$ Hz), 3.72 (t, 2H, $^3J = 8.0$ Hz), 4.12 (d, 2H, $^2J = 12.5$ Hz), 4.34 (d, 2H, $^2J = 12.5$ Hz), 4.86 (s, 2H), 4.95 (s, 4H), 6.80 (m, 4H), 6.84 (s, 4H), 7.37–7.45 (m, 3H), 7.54–7.67 (m, 6H), 8.11 (d, 1H, $^3J = 8.0$ Hz), 8.20–8.33 (m, 5H), 8.61 (s, br, 1H), 8.82 (s, br, 2H). ^{13}C NMR ($CDCl_3$): δ 10.1, 23.1, 30.9, 31.0, 31.3, 31.4, 33.8, 33.9, 73.8, 74.1, 119.5, 119.7, 120.4, 120.5, 125.0, 125.1, 125.4, 127.7, 133.5, 133.7, 133.8, 137.4, 138.9, 139.0, 141.3, 141.4, 144.5, 145.2, 145.3, 149.7, 150.4, 151.9, 152.0, 153.2, 153.3, 153.6, 156.9, 157.1. Anal. calcd. for $C_{80}H_{83}Br_3N_6O_4$: C, 67.09; H, 5.84; N, 5.87. Found: C, 66.74; H, 5.64; N, 5.51. Mp

156–157°C. ESI-ToF/MS: 1433.5 ($[3+H]^+$, 100%), 1455.4 ($[3+Na]^+$, 55%).

5,11,17,23-Tetra(tert-butyl)-26,27,28-tris[6-ethoxycarbonyl-2,2′-bipyridine-5′-yl]-25-propoxycalix[4]arene (4)

A solution of **3** (180 mg, 0.126 mmol) and $[Pd(PPh_3)_2Cl_2]$ (10 mg, 0.014 mmol) in a mixture of 10 ml CH_2Cl_2, 10 ml EtOH and 10 ml Et_3N was heated to 80°C for 18 hours under a CO atmosphere. The solution was cooled to room temperature, after which the solvents were removed under reduced pressure and the resulting solid was purified by column chromatography (Al_2O_3, CH_2Cl_2/hexane, 50/50 to 80/20) followed by recrystallisation with a CH_2Cl_2/MeOH mixture and drying under vacuum to give compound **4** (170 mg, 0.12 mmol, 96%) as white crystals. $R_f = 0.36$, Al_2O_3, CH_2Cl_2/MeOH, 99.5/0.5. ^1H NMR ($CDCl_3$): δ 0.82 (t, 3H, $^3J = 7.5$ Hz), 1.06 (s, 18H), 1.07 (s, 9H), 1.09 (s, 9H), 1.46 (t, 9H, $^3J = 7.0$ Hz), 1.78–1.96 (m, 2H), 2.86 (d, 2H, $^2J = 12.5$ Hz), 3.03 (d, 2H, $^2J = 12.5$ Hz), 3.72 (t, 2H, $^3J = 7.5$ Hz), 4.04 (d, 2H, $^2J = 12.5$ Hz), 4.30 (d, 2H, $^2J = 12.5$ Hz), 4.48 (qd, 6H, $^3J = 7.0$ Hz), 4.90 (s, 2H), 5.01 (s, 4H), 6.73–6.78 (m, 8H), 7.57 (d, br, 1H, $^3J = 8.0$ Hz), 7.70 (d, br, 2H, $^3J = 8.0$ Hz), 7.81–7.93 (m, 3H), 8.02–8.10 (m, 3H), 8.34 (d, 1H, $^3J = 8.0$ Hz), 8.43–8.57 (m, 5H), 8.66 (s, br, 1H), 8.88 (s, br, 2H). ^{13}C NMR ($CDCl_3$): δ 10.1, 14.2, 15.0, 18.6, 23.2, 29.6, 31.1, 31.3, 33.7, 33.8, 61.6, 66.3, 66.5, 73.7, 74.0, 76.0, 76.9, 120.5, 120.6, 124.0 (2C), 124.6 (2C), 124.9, 125.0, 125.3, 133.6, 133.7, 133.8, 137.5, 137.6, 137.8, 144.4, 145.1, 145.2, 147.5, 147.6, 150.2, 150.4, 151.7, 151.9, 153.3, 154.2, 154.4, 156.1, 156.2, 165.2. Mp >160°C decomp. Anal. calcd. for $C_{89}H_{98}N_6O_{10}$: C, 75.72; H, 7.00; N, 5.95. Found: C, 75.50; H, 6.71; N, 5.71. ESI-ToF/MS: 1412.8 ($[4+H]^+$, 3%), 1434.8 ($[4+Na]^+$, 100%).

5,11,17,23-Tetra(tert-butyl)-26,27,28-tris[6-carboxy-2,2′-bipyridine-5′-yl]-25-propoxycalix[4]arene Trisodium Salt (LNa_3)

Compound **4** (170 mg, 0.121 mmol) was suspended in 5 ml MeOH and NaOH (44 mg, 1.10 mmol) in 5 ml water was added. The solution was heated to 80°C, resulting in the dissolution of the ester. After 30 min, a white compound formed. After 2 hours, the solution was cooled to room temperature, the solid was isolated by centrifugation and washed with water until the water extracts were neutral. The isolated solid was dried under reduced pressure to give $\mathbf{L}Na_3$ (100 mg, 0.071 mmol, 59%) as a white solid. Anal. calcd. for $C_{83}H_{83}N_6O_{10}Na_3{\cdot}2H_2O$: C, 69.73; H, 6.15; N, 5.88. Found: C, 69.60; H, 6.02; N, 5.75. Mp >230°C decomp. ESI-ToF/MS: 708.3 ($[\mathbf{L}Na_3 + H + Na]^{2+}$, 100%), 719.8 ($[\mathbf{L}Na_3 + 2Na]^{2+}$, 95%), 1349.7 ($[\mathbf{L}Na_3 - 2Na + 3H]$, 82%), 1393.7 ($[\mathbf{L}Na_3 + H]$, 74%).

Synthesis of the Lanthanide Complexes

[EuL]·3H₂O

$\mathbf{L}Na_3$ (25 mg, 0.018 mmol) was dissolved in 10 ml of a 50/50 CH_2Cl_2/MeOH mixture and $EuCl_3{\cdot}6H_2O$ (6.8 mg, 0.018 mmol) dissolved in 2 ml MeOH was added. 10 ml acetonitrile were added to the solution which was concentrated by heating under reduced pressure. A pale yellow solid formed and the solution was allowed to cool to rt. The solid was collected by centrifugation and dried under vacuum to give the complex (13.6 mg, 0.0046 mmol, 51%). Anal. calcd. for $C_{83}H_{83}O_{10}N_6Eu{\cdot}3H_2O$: C, 65.13; H, 5.86; N, 5.49. Found: C, 64.96; H, 5.68; N, 5.12. ES-MS (1.14×10^{-4} mol dm^{-3}, CH_2Cl_2/MeOH 1/1): $m/z =$ 1499.9 (29%, $[Eu\mathbf{L}{\cdot}Na]^+$), 1008.1 (59%, $[Eu_2\mathbf{L}_2{\cdot}Na_3]^{3+}$), 762.2 (100%, $[Eu\mathbf{L}{\cdot}Na_2]^{2+}$). IR (KBr pellet): $\nu =$ 2960(m), 2869 (w), 1638 (s), 1480 (w), 1458 (m), 1384 (m), 1363 (m), 1296 (w), 1260 (w), 1193 (w).

[GdL]·3H₂O

The complex was obtained as described for europium starting from $\mathbf{L}Na_3$ (20.4 mg, 0.015 mmol) and $GdCl_3{\cdot}6H_2O$ (5.5 mg, 0.015 mmol) giving a pale yellow powder (10.1 mg, 0.0033 mmol, 44%). Anal. calcd. for $C_{83}H_{83}O_{10}N_6Gd{\cdot}3H_2O$: C, 64.91; H, 5.84; N, 5.47. Found: C, 64.78; H, 5.75; N, 5.37. IR (KBr Pellet): $\nu =$ 2962 (m), 2870 (w), 1637 (s), 1480 (w), 1437 (w), 1382 (s), 1297 (w), 1260 (w), 1193 (m).

[TbL]·3H₂O

The complex was obtained as described for europium starting from $\mathbf{L}Na_3$ (25.0 mg, 0.018 mmol) and $TbCl_3{\cdot}6H_2O$ (6.9 mg, 0.018 mmol) giving a yellow powder (17.5 mg, 0.0057 mmol, 63%). Anal. calcd. for $C_{83}H_{83}O_{10}N_6Tb{\cdot}3H_2O$: C, 64.84; H, 5.83; N, 5.47. Found: C, 64.61; H, 5.70; N, 5.15. IR (KBr pellet): $\nu =$ 2959 (m), 2869 (w), 1650 (s), 1597 (m), 1479 (w), 1458 (m), 1433 (w), 1363 (s), 1297 (w), 1254 (w), 1193 (m).

X-ray Crystal Structure Determination of [Tb₂L₂]

Crystal Data

$[TbC_{83}N_6O_{10}H_{83}]$, $2(CH_3CN)$, $3(CH_3OH)$, $2(H_2O)$. $M = 1697.74$, triclinic, space group $P\overline{1}$. Cell parameters: $a = 14.258(6)$; $b = 15.738(6)$; $c = 22.806(9)$ Å; $\alpha = 82.20(3)$; $\beta = 77.28(3)$; $\gamma = 82.34(3)°$, $Z = 2$, $\lambda =$ 0.947 Å. Crystallization of the complex gave micro diamond shaped plates, about 10 to 20 μm thick, the large dimension never exceeding 50 μm. These crystals are highly mosaic and have a general

TABLE I Summary of crystal data, intensity measurements and structure refinement for the Tb_2L_2 complex

Formula	$[Tb\ C_{83}O_{10}N_6H_{83}]$, $2(CH_3CN)$, $3(CH_3OH)$, $2(H_2O)$
Mol. wt.	1697.74
Crystal system	Triclinic
Space group	$P\bar{1}$
a, Å	14.258(6)
b, Å	15.738(6)
c, Å	22.806(9)
α, deg	82.20(3)
β, deg	77.28(3)
γ, deg	82.34(3)
V, Å^3	4917.4
Z	2
$F(000)$	1772
$D_c/\mathrm{Mg\,m^{-3}}$	1.147
$\mu(\lambda = 0.947)$, $\mathrm{mm^{-1}}$	0.779
Crystal size, mm	0.01 × 0.03 × 0.05
T, K	277
No. of reflns. collected	18128
θ range, deg	$5.97 < 2\theta < 25.36$
hkl ranges	$-12 \leq h \leq 12$
	$-13 \leq k \leq 14$
	$0 \leq l \leq 20$
No. of unique reflns.	5105
No. of reflns. obsd. $I > 2\sigma(I)$	5019
No. of parameters/restraints	1045/30
$R_1[I > 2\sigma(I)]^a$	0.1090
Weight	$1/[\sigma^2(F_o^2) + (0.1030)P^2 + 144.62P]^b$
wR_2^c	0.28
Max Fourier diff., e/Å^3	0.78, −0.87

$^a R_1 = \Sigma||F_o| - |F_c||/\Sigma|F_o|$. $^b P = (F_o^2 + 2F_c^2)/3$. $^c wR_2 = \{\Sigma[w(F_o^2 - F_c^2)^2]/\Sigma[w(F_o^2)^2]\}^{1/2}$.

tendency to twinning. As they are unstable upon exposure to air, they were transferred in Lindmann capillaries with a drop of the mother liquor. A microcrystal randomly oriented was used for the complete X-ray diffraction data recording at the DW-32 station on the wiggler line at the synchrotron DCI (Orsay) using a MAR345 image plate system at $\lambda = 0.964$ Å [14]. A full 360° rotation was recorded (72 frames 5 degree rotation each). Due to geometric restrictions, the resolution at the edge of the detector was reduced to 1.01 Å.

Data Reduction

The DENZO program from the HKL suite [15] was able to index the major component of the twinning. This allowed the integration of a complete set of 18128 reflections which were subsequently formatted in a suitable form for the CCP4 suite of programs [16]. After final reduction and merging ($R_{\mathrm{sym}} = 0.095$ on intensities), the data consisted of 5105 reflections of which 5019 were considered to be observed [with $F_o \geq 4\sigma(F_o)$]. The structure was solved by application of the Patterson function (SHELXS86) [17] and refined anisotropically on F^2 using all reflections by least-squares procedures [18]. Because of the paucity of the data versus the number of parameters to refine, restraints were applied to a selected set of bond distances and angles. Hydrogen atoms were modelled at their theoretical places using an isotropic thermal factor equal to 1.2 times that of the bonded atom. Due to high thermal parameters, no attempt was made to localize hydrogen atoms on solvent molecules. Crystallographic data and structure refinement details are given in Table I. A selection of the bond lengths and angles is reported in Table II. Structural data have been deposited with the Cambridge Crystallographic Data Centre (CCDC), reference no. 166824.

RESULTS AND DISCUSSION

Synthesis

The preorganized calix[4]arenes scaffoldings appear to be easily accessible compounds with interesting conformational, physicochemical and complexation properties [19]. As part of our own investigations on the utilization of these platforms as shaping units we first induced chemical modification of the lower rim of calixarenes with neutral bipyridine subunits [20]. Herein, the monoprotected calix[4]arene **2** [13] was chosen as a model compound for grafting on three anionic arms. The choice of the propyl chain as a fourth functionality on the calix[4]arene scaffold, was motivated by the possibility of changing it into a propylphthalimidate chain [21], with further potentialities for linking to biomolecules. Ligand **L** was obtained in three synthetic steps starting from **2** as depicted in Scheme 2. Deprotonation by NaH in dry

TABLE II Selected bond lengths (Å) and angles (°) for $Tb_2\mathbf{L}_2$

Tb–O(8A)	2.35(2)
Tb–O(8C)	2.37(2)
Tb–O(8B)	2.40(2)
Tb–N(1A)	2.51(2)
Tb–N(1C)	2.54(2)
Tb–N(1B)	2.62(3)
Tb–N(10C)	2.66(2)
Tb–N(10A)	2.69(2)
Tb–N(10B)	2.73(2)
O(8A)–Tb–O(8C)	87.8(6)
O(8A)–Tb–O(8B)	75.2(6)
O(8C)–Tb–O(8B)	142.7(5)
O(8A)–Tb–N(1A)	67.1(7)
O(8C)–Tb–N(1A)	72.5(5)
O(8B)–Tb–N(1A)	70.3(5)
O(8A)–Tb–N(1C)	71.4(6)
O(8C)–Tb–N(1C)	65.6(5)
O(8B)–Tb–N(1C)	134.5(6)
N(1A)–Tb–N(1C)	120.8(6)
O(8A)–Tb–N(1B)	131.9(7)
O(8C)–Tb–N(1B)	139.8(7)
O(8B)–Tb–N(1B)	61.7(8)
N(1A)–Tb–N(1B)	113.0(6)
N(1C)–Tb–N(1B)	126.0(6)
O(8A)–Tb–N(10C)	80.6(6)
O(8C)–Tb–N(10C)	128.5(5)
O(8B)–Tb–N(10C)	81.8(5)
N(1A)–Tb–N(10C)	141.3(8)
N(1C)–Tb–N(10C)	63.2(6)
N(1B)–Tb–N(10C)	73.4(6)
O(8A)–Tb–N(10A)	129.4(7)
O(8C)–Tb–N(10A)	70.5(5)
O(8B)–Tb–N(10A)	94.9(6)
N(1A)–Tb–N(10A)	62.9(9)
N(1C)–Tb–N(10A)	130.2(6)
N(1B)–Tb–N(10A)	77.2(6)
N(10C)–Tb–N(10A)	148.2(7)
O(8A)–Tb–N(10B)	147.9(6)
O(8C)–Tb–N(10B)	85.7(7)
O(8B)–Tb–N(10B)	125.5(7)
N(1A)–Tb–N(10B)	139.1(7)
N(1C)–Tb–N(10B)	77.3(7)
N(1B)–Tb–N(10B)	64.0(8)
N(10C)–Tb–N(10B)	79.1(6)
N(10A)–Tb–N(10B)	77.4(7)

DMF, followed by reaction with 6-bromo-5′-bromomethyl-2,2′-bipyridine **1**, afforded the tris(6-bromobipyridyl) compound **3** in a moderate yield.

Unfortunately, even under these conditions, in the presence of a large excess of base, complete deprotonation of the phenol moieties was difficult to achieve. Portionwise addition of the base and long reaction times led to improved yields but undesirable side reactions often occurred leading to impractical product mixtures. One-pot deprotonation and *O*-alkylation provide the most efficient alternative to the stepwise grafting of bipy units. Nevertheless, after an ethoxycarbonylation step where **3** is heated in a Et_3N/EtOH mixture containing $[Pd(PPh_3)_2Cl_2]$ as a catalyst with bubbling CO, the ester **4** was obtained in 96% yield. Saponification of **4** with NaOH in a MeOH/H_2O solution gave the target ligand as its trisodium salt (59%). Interestingly, while compounds **3** and **4** are very soluble in most chlorinated solvents, protic solvents such as MeOH or DMSO are required for solubilization of the triacid **L** or its anionic forms, thus showing improved hydrophilicity of the final compounds.

The NMR spectra of the intermediates are of particular interest with regard to their conformational structures. The ^1H NMR spectra of both compounds **3** and **4** display two AB spin system for the methylene bridging the phenolic units, with more than one ppm shift between the axial and equatorial protons, which unambiguously points to a cone conformation [22]. The presence of a vertical plane of symmetry passing through the *z* axis of the calixarene and containing the phenolic oxygen atom functionalized with the propyl chain induced an overall C_s symmetry group, further confirmed by the observation of two sets of protons for the bipyridyl subunit with relative intensities of 1:2. The methyl groups of the *tert*-butylphenols appeared as three singlets with relative intensities of 1:2:1. This conformational assignment is perfectly correlated with the ^{13}C NMR spectra, in which no peaks corresponding to methylene carbon atoms could be observed above 34 ppm. According to the work described by de Mendoza *et al.* [23], the presence of phenol rings in an *anti* conformation (such as the partial cone and the 1,3-alternate forms) is authenticated by chemical shift values around 37 ppm for the corresponding methylene bridges, which is clearly not the case here. Although $\mathbf{L}Na_3$ can hardly be identified by NMR spectroscopy, which showed only broad peaks in the expected regions, its identification was unambiguously established by high resolution

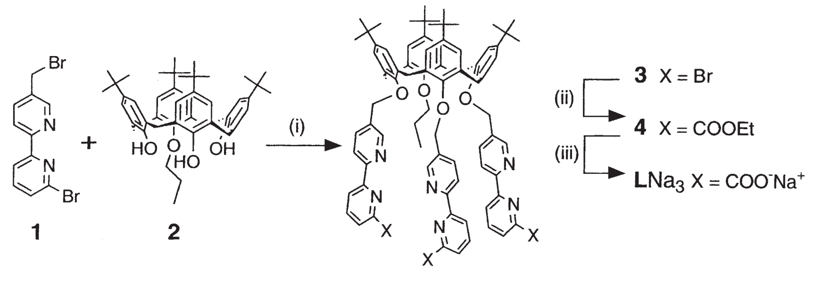

SCHEME 2 (i) DMF, NaH, rt, then **1** at 80°C in CH_3CN, (ii) $[Pd(PPh_3)_2Cl_2]$ (3 mol%), Et_3N, EtOH, CO (1 atm), 70°C, (iii) NaOH, MeOH, H_2O, 60°C.

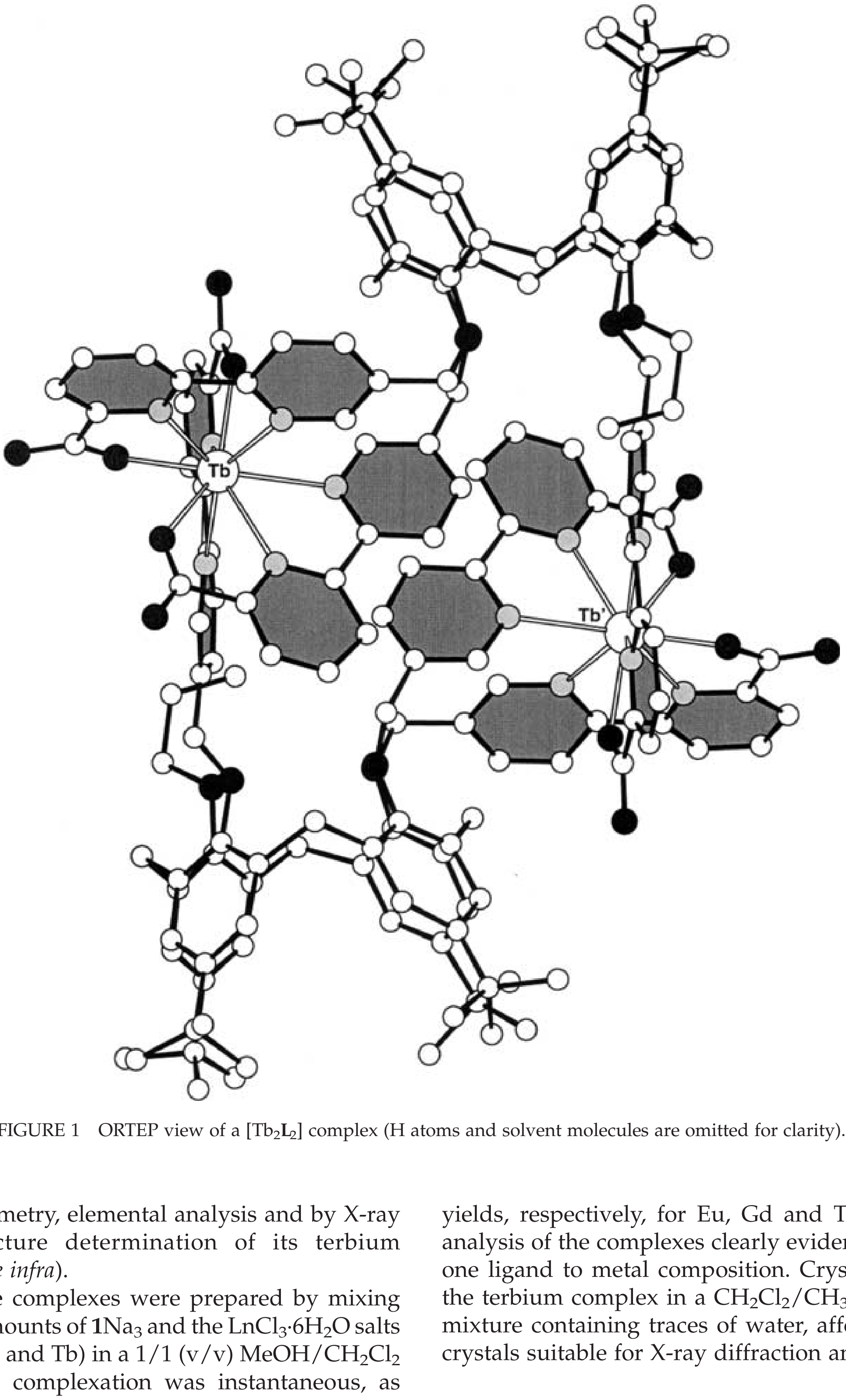

FIGURE 1 ORTEP view of a $[Tb_2\mathbf{L}_2]$ complex (H atoms and solvent molecules are omitted for clarity).

mass spectrometry, elemental analysis and by X-ray crystal structure determination of its terbium complex (*vide infra*).

Lanthanide complexes were prepared by mixing equimolar amounts of $\mathbf{1}Na_3$ and the $LnCl_3{\cdot}6H_2O$ salts (Ln = Eu, Gd and Tb) in a 1/1 (v/v) $MeOH/CH_2Cl_2$ mixture. The complexation was instantaneous, as evidenced by the appearance of a strong red emission (for Eu), upon irradiation with a conventional UV lamp. These complexes were soluble in $CH_2Cl_2/MeOH$ 1/1 mixtures but insoluble in acetonitrile or water. Recrystallisation of the complexes from $CH_2Cl_2/MeOH/CH_3CN$ mixtures afforded pale yellow solids with 51, 46 and 66% yields, respectively, for Eu, Gd and Tb. Elemental analysis of the complexes clearly evidenced a one to one ligand to metal composition. Crystallization of the terbium complex in a $CH_2Cl_2/CH_3CN/CH_3OH$ mixture containing traces of water, afforded monocrystals suitable for X-ray diffraction analysis.

X-ray Crystal Structure of the Terbium Complex

Description of the Structure

The X-ray structure of the Tb(III) compound revealed a dimeric $[Tb_2\mathbf{L}_2]$ complex. This complex crystallizes in the *P*-1 space group providing a neutral

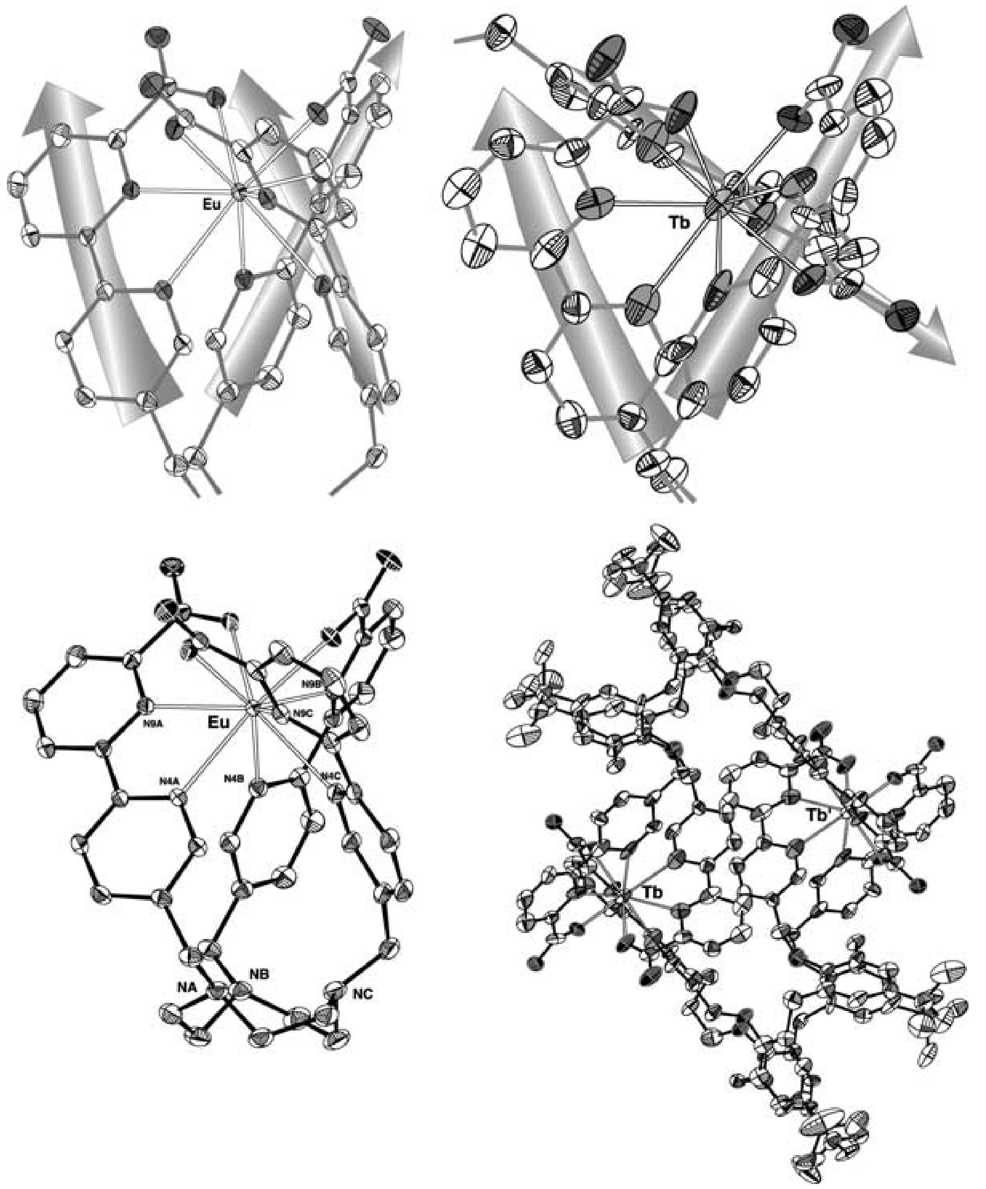

FIGURE 2 The coordination around lanthanides in [Eu**L**′] and [Tb_2**L_2**] structures. Bottom: ORTEP views of both structures. Top: Close up views of the coordination sphere around a single Ln atom. The arrows indicate orientations around the three bipyridine arms as connected from the different templates. This forms a "triple helix" in [Eu**L**′] and a "bowl" shaped motif in [Tb_2**L_2**].

centrosymmetric dinuclear species as shown in Fig. 1. The asymmetric unit consists of one calix[4]arene tridentate ligand **L**, one terbium(III) atom, two acetonitrile, three methanol and two water molecules present as solvates and which contribute to the cohesion of the crystal packing. As usually found for lanthanides, the rare earth atom displays nine coordination with formation of a favored tricapped prism. The coordination environment around each Tb(III) center consists of three tridentate bipyridine carboxylate units, two of them being provided by one calixarene, while the third one came from a second ligand. The distances and angles of the ligands surrounding the first coordination sphere are reported in Table II. The three Tb–O bond distances are 2.37 ± 0.03 Å, in good agreement with those reported for a related mononuclear europium complex with bipyridine carboxylate arms grafted onto a 1,4,7-triazacyclononane platform [24]. The six Tb–N bond distances are slightly different according to the nitrogen involved in the coordination: slight lengthening is observed for the N-binding of the pyridine ring connected to the calixarene template (2.69 ± 0.04) versus that of the pyridine ring linked to the carboxylate function (2.55 ± 0.07 Å).

Beyond the sphere of coordination the arrangement of the ligand displays a hitherto unknown construction. Unlike the crystalline structure of

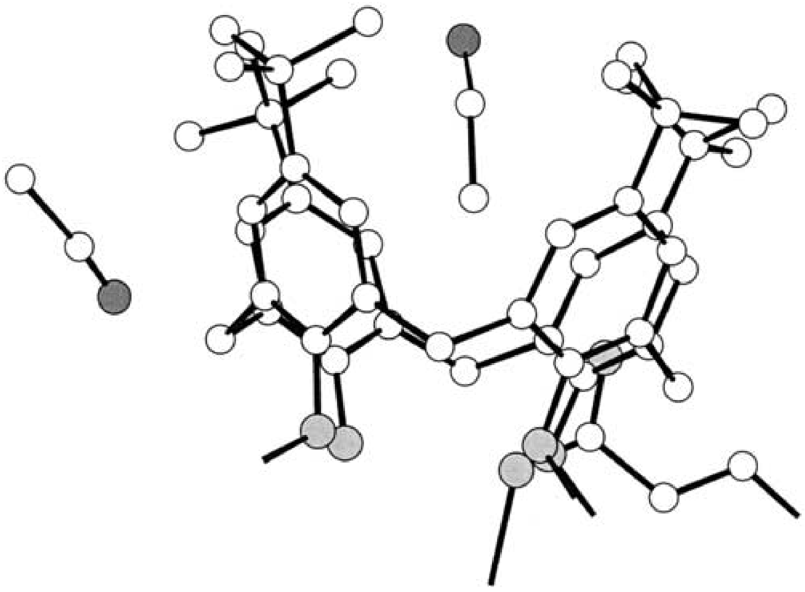

FIGURE 3 ORTEP view of the two molecules of acetonitrile in $[Tb_2\mathbf{1}_2]$. One molecule is trapped by the calix[4]–arene moiety, the second has more degrees of freedom in the packing.

the europium complex with three analogous chelating subunits but connected to another template (Fig. 2) [24], the monomeric nature of the molecular unit is not present in the terbium complex. It is likely that steric hindrance around the calixarene shaping unit forces the bipy-carboxylate subunits to fold around the main axis. Two of these units come from a single ligand while the third comes from an additional ligand. A symmetrical arrangement occurs for the second terbium thus building a dimeric complex in the solid state (Fig. 1) instead of the expected monomeric complex. In the previous Eu(III) structure, the wrapping of the three bipyridine subunits around the Eu(III) ion leads to the formation of a propeller like structure (of a triple helix type) with a pseudo C_3 inner symmetry, the N,N,COO$^-$ frames forming an angle of 121 ± 5° with the mean plane defined by the macrocycle. In the present Tb(III) structure, because of the spatial origin of the three anionic arms, this C_3 symmetry is broken as shown in Fig. 2. As a consequence, the planarities of the bipyridine subunits display slight differences to accommodate this new conformation, with tilt angles of the two adjacent pyridine rings of, respectively, 14(1)°, 15(1)° and 20(1)° for the three different arms. The angles between the mean planes of the three bipyridine arms are 85 ± 4°.

TABLE III Geometric parameters of H-bonds

Acceptor	Donor	Distance
O9A [*x*, *y*, *z*]	O2 [−1+*x*, *y*, *z*]	2.66(3) Å
O9C [*x*, *y*, *z*]	O1 [*x*, *y*, *z*]	2.78(2) Å
O9A [1+*x*, *y*, *z*]	O2 [*x*, *y*, *z*]	2.66(3) Å
O2 [*x*, *y*, *z*]	O3 [1 − *x*, 1 − *y*, −*z*]	2.78(4) Å
		Angle
	Me1–O1······O9C	102(1)°
	(*x*, *y*, *z*) (*x*, *y*, *z*)	
	Me2–O2······O3	122(3)°
	(*x*, *y*, *z*) (*x*, *y*, *z*) (1 − *x*, 1 − y, −*z*)	
	Me2–O2······O9A	99(2)°
	(*x*, *y*, *z*) (*x*, *y*, *z*) (1+*x*, *y*, *z*)	
	O3············ O2············ O9A	126(2)°
	(1 − *x*, 1 − *y*, 1 − *z*) (*x*, *y*, *z*) (1+*x*, *y*, *z*)	

Solvation and Stabilization of the Packing

The supramolecular structure includes a number of solvent molecules coming from the mother liquor used in the crystallization of the complex (mixture of dichloromethane, acetonitrile, methanol and water coming from the salts). The metal atoms are well protected from solvent molecules, which are relegated away from the first coordination sphere. The calix[4]arene macrocycles are in a cone conformation with an acetonitrile molecule being trapped in the conical cavity, as is often observed with calixarene structures (Fig. 3) [25,26]. The additional acetonitrile molecule just fills a cavity in the packing of the molecules in the solid phase. Interestingly, the methanol molecules which co-crystallized are basically involved in a supramolecular H-bonded network. Two of the three oxygen atoms of the carboxylate subunits, not coordinated with the terbium atoms, and the three

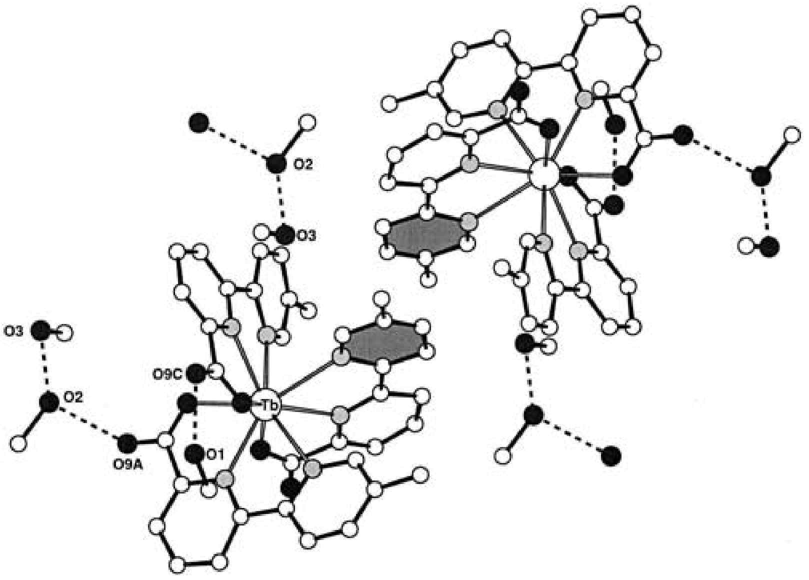

FIGURE 4 ORTEP drawing of the two centrosymetrically related coordination cores of Tb(III). The calixarene groups are removed for clarity. This illustrates the hydrogen bond net connecting the methanol molecules and the free carboxylate oxygen atoms.

methanol molecules are H-bonded through linear or twofold hydrogen bonds (Table III and Fig. 4). Two additional peaks were modelled as water molecules as they lie in channels of the molecular packing. It is worth pointing out that a stacking association involving two pyridine rings belonging to the two different calix[4]arene of the same dimeric unit is clearly evidenced (Fig. 4). These

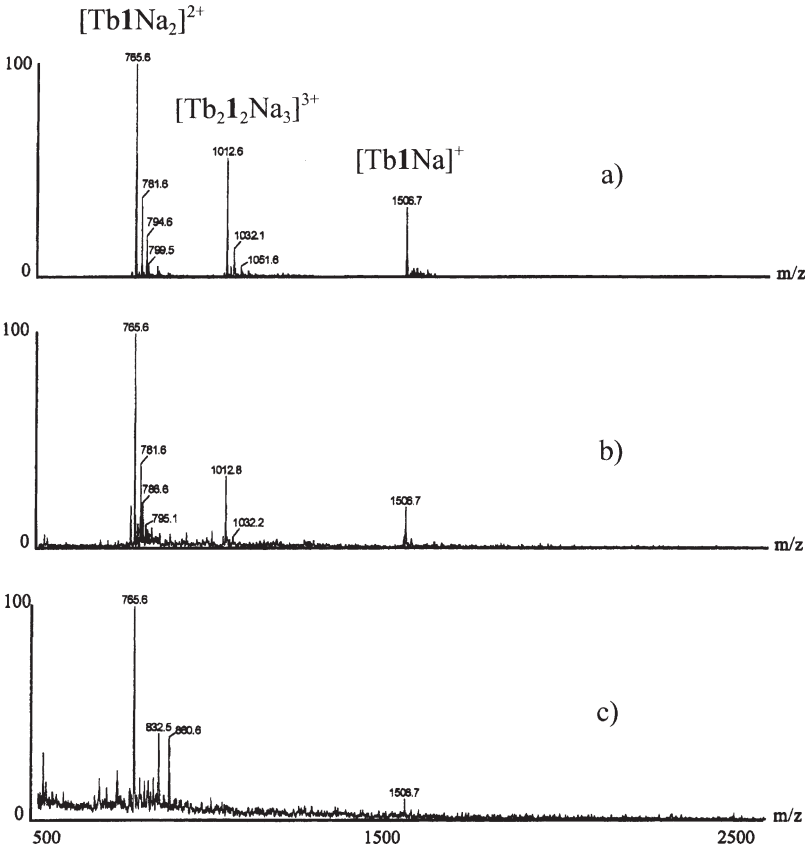

FIGURE 5 ES-MS spectra of 1.73×10^{-4} (a), 1.73×10^{-5} (b) and 1.73×10^{-6} (c) mol dm^{-3} solutions of $[Tb_2\mathbf{L}_2]$ in 1/1 (v/v) MeOH/CH_2Cl_2 solutions.

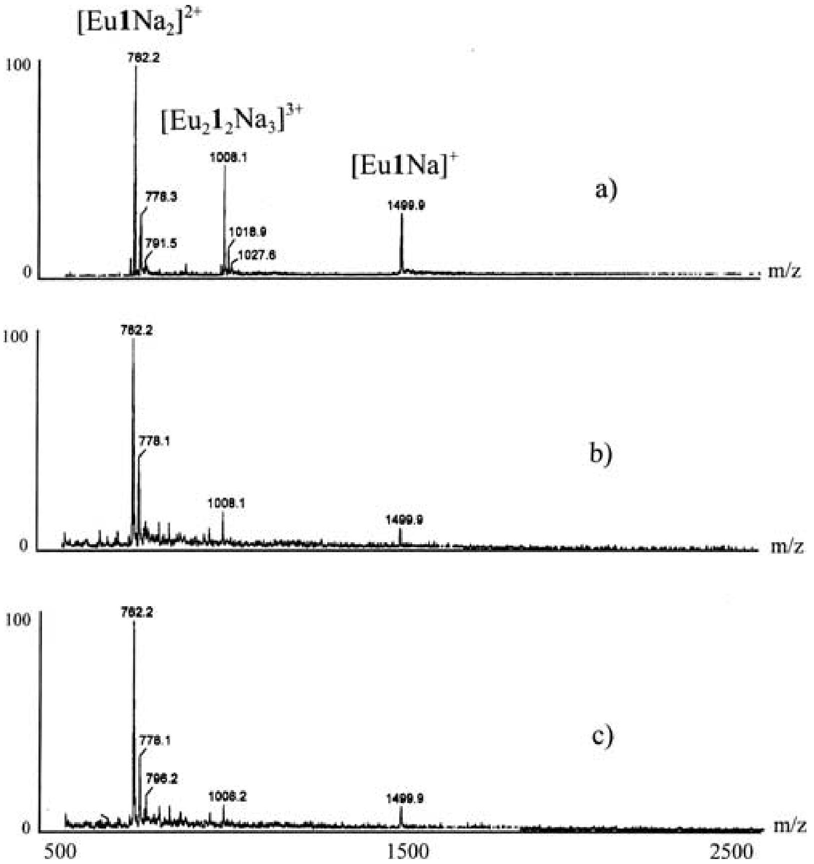

FIGURE 6 ES-MS spectra of 1.14 × 10^{-4} (a), 1.14 × 10^{-5} (b) and 1.14 × 10^{-6} (c) mol dm^{-3} solutions of [Eu$_2$**L**$_2$] in 1/1 (v/v) MeOH/CH$_2$Cl$_2$ solutions.

pyridine rings are related by a symmetry centre and exhibit strong π–π stacking (mean distance 3.7 Å) and this interaction contributes to the overall stability of the scaffold.

Solution Behavior

NMR spectra of the Eu and Tb complexes were poorly resolved and displayed broad signals that were difficult to assign. The paramagnetic contributions of the lanthanide cations on the one hand and exchange phenomenon on the other hand, are probably responsible for such behavior. We then turned our attention toward the use of ES-MS spectrometry to gain better insight into the species present in solution. The ES-MS spectrum of a solution of the Tb complex in 1/1 (v/v) CH$_2$Cl$_2$/MeOH solution at a concentration of 1.73 × 10^{-4} mol dm^{-3} displayed three major peaks (Fig. 5) which were unambiguously assigned by high resolution experiments. A triply charged species ($m/z = 1012.6$, 56%) corresponding to [Tb$_2$**L**$_2$·Na$_3$]$^{3+}$ confirmed the presence of the dimeric structure in solution (Scheme 1). Two other peaks corresponding to monometallic species [Tb**L**·Na$_2$]$^{2+}$ ($m/z = 765.6$, 100%) and [Tb**L**·Na]$^+$ ($m/z = 1506.7$, 32%) were also observed. Ascertaining whether these two peaks correspond to the presence of a monometallic species in solution or to fragmentation of [Tb$_2$**L**$_2$] was addressed using measurements at different concentrations. After an initial tenfold dilution of the sample, the relative intensities of the peaks changed to 100:34:19 (respectively for [Tb**L**·Na$_2$]$^{2+}$, [Tb$_2$**L**$_2$·Na$_3$]$^{3+}$ and [Tb**L**·Na]$^+$) and a second tenfold dilution (final concentration of 1.73 × 10^{-6} mol dm^{-3}) led to 100: < 7:10, while keeping the measurement parameters unchanged. This evolution is well understood in terms of a dissociation equilibrium in which the [Tb$_2$**L**$_2$] species dissociates to form the [Tb**L**] species which becomes the major product at high dilution. Similar behavior was observed for the europium complex (Fig. 6). At a concentration of 1.14 × 10^{-4} mol dm^{-3} the three peaks corresponding to [Eu**L**·Na$_2$]$^{2+}$ ($m/z = 762.2$, 100%), [Eu$_2$**L**$_2$·Na$_3$]$^{3+}$ ($m/z = 1008.1$, 59%) and [Eu**L**·Na]$^+$ ($m/z = 1499.9$, 29%) were observed. High resolution experiments allows the unambiguous assignment of the charge of the peaks (Fig. 7). Two tenfold dilutions led to relative intensities of 100:37:16 and 100:13:12, successively, also pointing to the decrease of the concentration of the dimeric species.

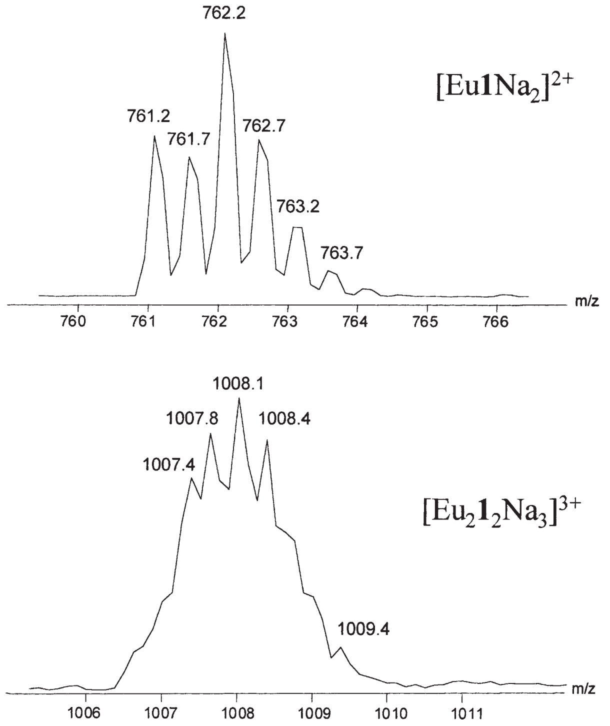

FIGURE 7 High resolution ES-MS spectra of a 1.73×10^{-4} mol dm^{-3} solution of [Eu_2**L_2**] in a 1/1 (v/v) $MeOH/CH_2Cl_2$ solution.

Photophysical Properties

The absorption spectra of the lanthanide complexes of ligand **L** in $CH_2Cl_2/MeOH$ 1/1 (v/v) solution are characterized by intense absorption bands in the UV region, which are attributed to $\pi-\pi^*$ transitions of the 2,2′-bipyridine (bpy) moieties (Table IV and Fig. 8). The intensities of the absorption bands are consistent with the presence of six bpy chromophores in the complex. Under UV irradiation both the Eu and Tb complexes showed metal luminescence due to an energy transfer process from the excited ligand to the metal emitting state, as demonstrated by the similarity between the metal luminescence excitation and the ligand absorption spectra (Fig. 8).

Deconvolution of the metal luminescence decay profiles for the Eu complex revealed a double exponential decay, with lifetimes of 0.75 and 2.3 ms, in agreement with the presence of two distinct Eu species as previously observed by ES-MS experiments. An examination of the concentration dependence of the pre-exponential terms in the range 3.0×10^{-5} to 1.0×10^{-6} mol dm^{-3} showed the concentration of the species with the longer lifetime to decrease with dilution (see Fig. 9). The correlation with ES-MS results allowed us to attribute this longer lifetime to the [Eu_2**L_2**] species. Furthermore, the value of 2.3 ms is in good agreement with that measured for a similar complex of Eu protected by three bpy-carboxylate arms (1.85 ms in water at room temperature) [24], although it was not measured in the same solvent. This indicates that the metal atom is quite well protected from interactions with solvent molecules and that the structure of the solid sample (in which each europium ion is coordinated to three bpy moieties) is probably kept in solution. The shorter lifetime was attributed to the [Eu**L**] species and may be related to decoordination of one bpy arm, as would be anticipated during the formation of [Eu**L**] following dismutation of [Eu_2**L_2**], or to a less favourable coordination geometry in the monometallic species due to steric constraints resulting in a less efficient shielding of the metal ion from the environment.

A similar bi-exponential decay was also observed for the Tb complex with lifetimes of 0.07 and 1.0 ms in the same solvent mixture (data not shown). However, the concentration-dependent behavior of the pre-exponential terms suggests that the dimetallic [Tb_2**L_2**] species possesses a shorter lifetime than the monometallic one. Although somewhat surprising, these results are in agreement with data showing that the complexation of a third bpy-COO^- arm to a terbium ion should be detrimental to the excited state lifetime. When two 5′-methyl-6-carboxylato-2,2′-bipyridine arms are complexed on a Tb^{3+} ion, with two water molecules and an hydroxide anion completing the first coordination sphere, the excited state lifetime of the metal was measured to be 0.80 ms in water [27]. This value falls to 0.50 ms when the coordination sphere is made up of three bpy-COO^- arms in the same solvent [24]. It should be noted that metal excited state lifetimes of the corresponding Eu complexes showed the reverse trend: the lifetime increased from 0.30 ms to 1.85 ms when a third bpy-carboxylate arm coordinated the metal ion.

TABLE IV Photophysical data for the lanthanide complexes of ligand **L**[a]

	Absorption		Metal luminescence[b]	
Lanthanide complex	λ_{max}/nm	$\varepsilon_{\lambda max}$/dm^3 mol^{-1} cm^{-1}	τ/ms	Φ
Eu	309	71500	0.75, 2.3[c]	0.017
Tb	308	67000	0.07, 1.0[c]	~0.001
Gd	309	66000	[d]	[d]

[a] Data obtained in aerated $CH_2Cl_2/MeOH$ 1/1 (v/v) solution at room temperature ($c = 1.0 \times 10^{-5}$ mol dm^{-3}, assuming a [Ln_2**L_2**] formula). [b] Upon excitation of the ligand absorption at 309 nm. [c] Lifetimes obtained by a double exponential fitting of the metal luminescence decay. [d] No metal luminescence was observed.

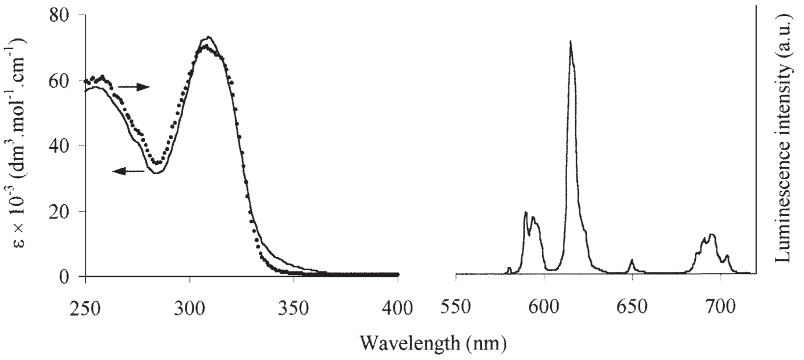

FIGURE 8 Left panel: absorption (continuous line) and metal luminescence excitation (dotted line) spectra obtained for the [$Eu_2\mathbf{L}_2$] complex in CH_2Cl_2/MeOH 1/1 (v/v) solution. Right panel: metal luminescence emission spectra obtained for [$Eu_2\mathbf{L}_2$] upon excitation of the ligand absorption.

This opposite behavior of europium and terbium could be rationalized by considering the different nature of the main deactivation processes of the metal emitting states. While deactivation of the Eu emitting states usually take place by vibronic coupling with coordinated solvent molecules, the most common non-radiative deactivation process in Tb complexes with ligands containing bpy moieties is back energy transfer to ligand triplet excited states. The coordination of the third bpy arm is suspected to move the ligand centered triplet excited state toward lower energy, thereby favoring back energy transfer in the case of the terbium complexes, while it allows for better shielding of the metal with concomitant decrease of non-radiative deactivation for europium.

The metal luminescence quantum yields measured following excitation into the ligand were relatively low, particularly in the case of the Tb complex (Table IV). It should be pointed out, however, that the measured quantum yields only represent mean values because of the presence of different metal-containing species in solution. Anyway, at least for the Eu species, the long luminescence lifetimes suggest that deactivation processes of the metal emitting state are relatively inefficient, so that the low quantum yields may indicate a low ligand-to-metal energy transfer efficiency.

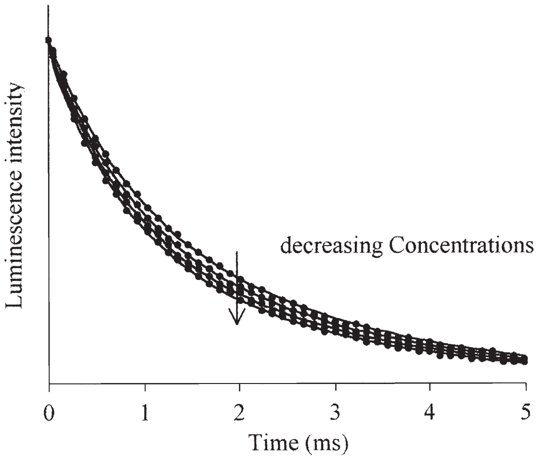

FIGURE 9 Metal luminescence decay profiles measured for the [$Eu_2\mathbf{L}_2$] complex in CH_2Cl_2/MeOH 1/1 (v/v) solution in the 3.0×10^{-5} (upper profile) to 1.0×10^{-6} (lower profile) mol dm^{-3} concentration range (all the decay profiles were normalized to the same initial intensity). The lines represent the results of the fitting of the decay profiles by a double exponential equation, in which the lifetimes were kept constant at 0.75 and 2.3 ms; upon dilution, the ratio between the preexponential terms associated with the short and long lifetime components varied from 0.3 to 0.8.

CONCLUSIONS

We have developed a tri-anionic ligand using a calix[4]arene as a shaping unit which binds lanthanide(III) cations to form 1:1 and 2:2 (M:L) complexes in a concentration-dependent equilibrium. In this ensemble the photophysical data suggested that the cations in the dimeric species are fairly well protected from the solvent and coordinated to three 6-carboxylatobipyridyl arms, similar to the situation in the solid state structure of the terbium dimer, while coordination is less efficient in the monometallic species. We are currently investigating methods for selectively derivatizing this scaffold with other anionic chelating arms in order to better control the coordination process, the nuclearity of the final complex and the solubility in aqueous media.

Acknowledgements

We thank the Centre National de la Recherche Scientifique and the French Ministère des Affaires Etrangères (Projet Galilée) for financial support, the MURST (Ministero dell'Università e della Ricerca Scientifica e Tecnologica, Italy) and the CRUI (Conferenza dei rettori delle Università Italiane, Progetto Galileo).

References

[1] Sabbatini, N.; Guardigli, M.; Manet, I.; Ziessel, R. In *Calixarenes 2001*; Asfari, Z., Böhmer, J. V., Harrowfield, J., Vicens, J., Eds.; Kluwer Academic Publishers: Dordrecht, The Netherlands, 2001; Chap. 31, p 583.

[2] Dozol, J. F.; Lamare, V.; Simon, N.; Ungaro, R.; Casnati, A. In *Calixarenes for Separation*, Lumetta, G. J., Rogers, R. D., Gopalan, A., Eds.; American Chemical Society: Washington DC, 2000, Vol. 757, Chap. 2, p 12.

[3] Yaftian, M. R.; Burgard, M.; Matt, D.; Dieleman, C. B.; Rastegar, F. *Solv. Extr. Ion Exch.* **1997**, *15*, 975.

[4] Steemers, F. J.; Verboom, W.; Reinhoudt, D. N.; van der Tol, E. B.; Verhoeven, J. W. *J. Am. Chem. Soc.* **1995**, *117*, 9408.

[5] Prodi, L.; Pivari, S.; Boletta, F.; Hissler, M.; Ziessel, R. *Eur. J. Inorg. Chem.* **1998**, 1959.

[6] Piguet, C.; Bünzli, J.-C. G. *Chem. Soc. Rev.* **1999**, *28*, 347.

[7] *Applications of Fluorescence in Immunoassays*, Hemmilä, I., Ed.; Wiley: New York, 1991.

[8] Parker, D.; Kanthi-Senanayake, P.; Williams, J. A. G. *J. Chem. Soc. Perkin Trans.* **1998**, *2*, 2129.

[9] Kido, J.; Ikeda, W.; Kimura, M.; Nagai, K. *Jpn. J. Appl. Phys.* **1996**, *35*, 394.

[10] Georgiev, E. M.; Clymire, J.; McPherson, G. L.; Roundhill, D. M. *Inorg. Chim. Acta* **1994**, *227*, 293.

[11] Sabbatini, N.; Guardigli, M.; Mecati, A.; Balzani, V.; Ungaro, R.; Ghidini, E.; Casnati, A.; Pochini, A. *J. Chem. Soc. Chem. Commun.* **1990**, 878.

[12] Charbonnière, L. J.; Weibel, N.; Ziessel, R. F. *Tetrahedron Lett.* **2001**, *42*, 659.

[13] Grigg, R.; Holmes, J. M.; Jones, S. K.; Amilaprasadh Norbert, W. D. J. *J. Chem. Soc. Chem. Commun.* **1994**, 185.

[14] Fourme, R.; Dhez, P.; Benoit, J. P.; Kahn, R.; Dubuisson, J. M.; Buisson, P.; Frouin, J. *Rev. Sci. Instrum.* **1992**, *63*, 982.

[15] Otwinosky, Z.; Minor, W. *Methods Enzymol.* **1997**, *276*, 307.

[16] CCP4 Collaboration Computational Project No. 4 *Acta Crystallogr. Sect. D* **1994**, *50*, 760.

[17] Sheldrick, G. M. *Acta Crystallogr. Sect. A* **1990**, *46*, 467.

[18] Sheldrick, G. M. *Program for the Refinement of Crystal Structures*; Universität Göttingen, 1993.

[19] *Calixarenes 2001*; Asfari, Z., Böhmer, V., Harrowfield, J., Vicens, J., Eds.; Kluwer Academic Publishers: Dordrecht, The Netherlands, 2001.

[20] Ulrich, G.; Ziessel, R.; Manet, I.; Guardigli, M.; Sabbatini, N.; Fraternali, F.; Wipff, G. *Chem. Eur. J.* **1997**, *3*, 1815.

[21] Matthews, S. E.; Parzuchowski, P.; Garcia-Carrera, A.; Grüttner, C.; Dozol, J.-F.; Böhmer, V. *Chem. Commun.* **2001**, 417.

[22] Gutsche, C. D., *Calixarenes, Monographs in Supramolecular Chemistry*; The Royal Society of Chemistry: Cambridge, 1992; Chap. 4.

[23] Jaime, C.; de Mendoza, J.; Prados, P.; Nieto, P. M.; Sànchez, C. *J. Org. Chem.* **1991**, *56*, 3372.

[24] Charbonnière, L. J.; Guardigli, M.; Cesario, M.; Roda, A.; Sabbatini, N.; Ziessel, R. *J. Am. Chem. Soc.* **2001**, *123*, 2436.

[25] Olmstead, M. M.; Sigel, G.; Hope, H.; Xu, X.; Power, P. P. *J. Am. Chem. Soc.* **1985**, *107*, 8087.

[26] Ramirez, F. de M.; Charbonnière, L.; Muller, G.; Scopelliti, R.; Bünzli, J.-C. *J. Chem. Soc. Dalton Trans.* **2001**, 3205.

[27] Lifetimes of 0.31 and 0.80 ms in water were obtained, respectively, for Eu and Tb salts complexed with two bpy-carboxylate ligands, two water molecules and a hydroxide anion. Charbonnière, L.J., Ziessel, R., Guardigli, M. Unpublished results.